

# Hypoxia promotes the phenotypic change of aldehyde dehydrogenase activity of breast cancer stem cells

Akira Shiraishi,<sup>1</sup> Kana Tachi,<sup>1,2</sup> Nesrine Essid,<sup>1</sup> Ikki Tsuboi,<sup>1</sup> Masumi Nagano,<sup>1</sup> Toshiki Kato,<sup>1,3</sup> Toshiharu Yamashita,<sup>1</sup> Hiroko Bando,<sup>2</sup> Hisato Hara<sup>2</sup> and Osamu Ohneda<sup>1</sup>

<sup>1</sup>Department of Regenerative Medicine and Stem Cell Biology, Graduate School of Comprehensive Human Sciences, University of Tsukuba, Tsukuba, Ibaraki; <sup>2</sup>Department of Breast-Thyroid-Endocrine Surgery, Institute of Clinical Medicine, University of Tsukuba, Tsukuba, Ibaraki; <sup>3</sup>Ph.D. Program in Human Biology, School of Integrative and Global Majors, University of Tsukuba, Tsukuba, Ibaraki, Japan

## Key words

Aldehyde dehydrogenase, breast cancer, cancer stem cells, epithelial-mesenchymal transition, hypoxia-inducible factor-1 $\alpha$

## Correspondence

Osamu Ohneda, Department of Regenerative Medicine and Stem Cell Biology, Graduate School of Comprehensive Human Sciences, University of Tsukuba, 1-1-1 Tennodai, Tsukuba, Ibaraki 305-8575, Japan.  
Tel: +81-29-853-2938; Fax: +81-29-853-2938;  
E-mail: oohneda@md.tsukuba.ac.jp

## Funding Information

Ministry of Education, Culture, Sports, Science, and Technology.

Received September 9, 2016; Revised December 15, 2016; Accepted December 20, 2016

*Cancer Sci* 108 (2017) 362–372

doi: 10.1111/cas.13147

Stable breast cancer cell (BCC) lines are valuable tools for the identification of breast cancer stem cell (BCSC) phenotypes that develop in response to several stimuli as well as for studying the basic mechanisms associated with the initiation and maintenance of BCSCs. However, the characteristics of individual, BCC-derived BCSCs varies and these cells show distinct phenotypes depending on the different BCSC markers used for their isolation. Aldehyde dehydrogenase (ALDH) activity is just such a recognized biomarker of BCSCs with a CD44<sup>+</sup>/CD24<sup>-</sup> phenotype. We isolated BCSCs with high ALDH activity (CD44<sup>+</sup>/CD24<sup>-</sup>/Aldefluor<sup>POS</sup>) from a primary culture of human breast cancer tissue and observed that the cells had stem cell properties compared to BCSCs with no ALDH activity (CD44<sup>+</sup>/CD24<sup>-</sup>/Aldefluor<sup>NEG</sup>). Moreover, we found Aldefluor<sup>POS</sup> BCSCs had a greater hypoxic response and subsequent induction of HIF-1 $\alpha$  expression compared to the Aldefluor<sup>NEG</sup> BCSCs. We also found that knocking down HIF-1 $\alpha$ , but not HIF-2 $\alpha$ , in Aldefluor<sup>POS</sup> BCSCs led to a significant reduction of the stem cell properties through a decrease in the mRNA levels of genes associated with the epithelial-mesenchymal transition. Indeed, HIF-1 $\alpha$  overexpression in Aldefluor<sup>NEG</sup> BCSCs led to Slug and Snail mRNA increase and the associated repression of E-cadherin and increase in Vimentin. Of note, prolonged hypoxic stimulation promoted the phenotypic changes of Aldefluor<sup>NEG</sup> BCSCs including ALDH activity, tumorigenesis and metastasis, suggesting that hypoxia in the tumor environment may influence BCSC fate and breast cancer clinical outcomes.

It has been reported that CD44 and CD24 are good markers to isolate cancer stem cells (CSC) subpopulations from breast cancer.<sup>(1)</sup> CD44<sup>+</sup>/CD24<sup>-low</sup> cells are more common in basal-like tumors and are strongly associated with BRCA1-mediated hereditary breast cancer but not all CD44<sup>+</sup>/CD24<sup>-low</sup> cells show a basal-like cell phenotype. Furthermore, not all CD44<sup>+</sup>/CD24<sup>-low</sup> populations in breast tumors are CSCs but rather are non-stem tumor cells, which have highly proliferative potential and lead to poor clinical outcomes.<sup>(2,3)</sup> On the other hand, aldehyde dehydrogenase (ALDH) was identified as specific marker that can be used to isolate stem cells from not only normal tissues, but malignant ones as well.<sup>(4)</sup> The ALDH phenotype correlated with clinical outcome; however, no association with a particular subtype of breast cancer cells (BCCs) was identified.<sup>(5)</sup> Ginestier and colleagues found that Aldefluor-positive (for ALDH activity) BCC populations in mice have a 1% or less overlap with the population of CD44<sup>+</sup>/CD24<sup>-low</sup> cells. Additionally, Aldefluor-positive and CD44<sup>+</sup>/CD24<sup>-low</sup> populations were reported to have high tumorigenic activity, including proliferation and tumor formation after transplantation of just 20 cells per recipient mouse.

Because stem cells divide asymmetrically, the cellular progeny exhibits a high degree of differentiation and neoplastic cells are therefore generally thought to be at various differentiated stages. Importantly, it has been reported that normal and cancer stem cell-like cells can arise *de novo* from cells at a more advanced differentiation stage, indicating that there are heterogeneous populations regulated by bidirectional interconversions.<sup>(6,7)</sup> Therefore, non-stem cancer cells give rise to CSCs due to an unexpected degree of plasticity. However, the mechanisms of phenotypic changes inducing CSCs have not been investigated in detail.

One of the key extrinsic effects on cancer cells is a hypoxic environment. Hypoxia-inducible factor-1 $\alpha$  (HIF-1 $\alpha$ ) is overexpressed and is associated with the proliferation of breast, lung, gastric, skin, ovarian, pancreatic, prostate and renal cancers.<sup>(8)</sup> Furthermore, it has been demonstrated that blocking HIF-1 $\alpha$  in breast cancers inhibits tumor growth, angiogenesis, stem cell maintenance, invasion and metastasis.<sup>(9)</sup> Increased expression of HIF-1 $\alpha$  is closely related to a poor prognosis and resistance to therapy in various types of cancers.<sup>(10)</sup> Hypoxia is also an important factor in the epithelial-mesenchymal transition (EMT) in breast cancer.<sup>(11)</sup> HIF-1 $\alpha$  binds to hypoxia response

elements (HRE) in the Snail and Slug promoters and increases their expression, while simultaneously decreasing the expression of E-cadherin, leading to the EMT and increased cancer aggressiveness.<sup>(12,13)</sup> These previous findings indicate that HIF-1 $\alpha$  induces cancer development in a variety of aspects, and it represents a key molecule involved in various cancer-related processes.

In this study, we isolated breast cancer stem cells (BCSCs) (CD44<sup>+</sup>/CD24<sup>-</sup>) with high ALDH activity (Aldefluor<sup>pos</sup>) from human breast cancer tissue and showed CD44<sup>+</sup>/CD24<sup>-</sup>/Aldefluor<sup>pos</sup> cells had greater stem cell properties and hypoxic response (as measured by induction of HIF-1 $\alpha$  expression) compared to CD44<sup>+</sup>/CD24<sup>-</sup>/Aldefluor<sup>neg</sup> cells. Furthermore, we found HIF-1 $\alpha$  to be highly involved in the generation of Aldefluor<sup>pos</sup> cells and induce Snail and Slug expression at both mRNA and protein levels, leading to the EMT phenotype. Moreover, we identified hypoxic induction of Aldefluor<sup>pos</sup> cells from Aldefluor<sup>neg</sup> cells and those altered Aldefluor<sup>pos</sup> cells expressed angiogenic genes rather than EMT-related genes. Indeed, when hypoxia-induced Aldefluor<sup>pos</sup> cells derived from Aldefluor<sup>neg</sup> stock were transplanted into mice, tumorigenic and metastatic activities increased significantly compared to controls and resembled the activity Aldefluor<sup>pos</sup> of cells at time zero.

## Materials and Methods

**Patient sampling and established cell lines (BC#1).** Human pleural effusion from a metastatic breast cancer patient (79 years of age, estrogen receptor [ER]-positive, progesterone receptor [PgR]-positive, human epidermal growth factor receptor 2 [HER2]-negative) was harvested from a surgical sample using a protocol approved by the ethics committee of the University of Tsukuba. Isolated cells (ER<sup>+</sup>/PgR<sup>+</sup>/HER2<sup>-</sup>) were plated on tissue culture dishes and expanded *in vitro*.<sup>(14)</sup> After expansion, CD45<sup>-</sup>/CD31<sup>-</sup>/CD44<sup>+</sup>/CD24<sup>-</sup> cells (BC#1) were segregated from the mixed population by FACS (MoFlo XDP; Beckman Coulter, Brea, CA, USA) and maintained with Dulbecco's modified eagle medium (DMEM)-high medium (Invitrogen, Carlsbad, CA, USA) containing 10% FBS, L-glutamine and MEM-NEAA (Invitrogen). We used early passages of BC#1 (up to passage number 8) for further experiments. We harvested and cultured four additional breast cancer cell batches derived from the pleural effusion of different patients, using the same protocol. One of these batches (BC#1) was maintained in the same culture condition as above. For control, MCF-7 (Riken BioResource Center, Ibaraki, Japan) and SK-BR-3 (ATCC #HTB-30<sup>TM</sup>; Manassas, VA, USA) were utilized.

**Antibodies for FACS.** The antibodies used in this study were phycoerythrin (PE)-labeled anti-CD24 (Biolegend, San Diego, CA, USA), fluorescein isothiocyanate (FITC)-labeled anti-CD44 (BD Biosciences, San Jose, CA, USA), allophycocyanine (APC)-labeled anti-E-cadherin (Biolegend) and PE-labeled anti-Vimentin (R&D systems, Minneapolis, MN, USA).

**Aldefluor assay.** Aldehyde dehydrogenase activity was analyzed with Aldefluor reagent (StemCell Technologies Inc, Vancouver, BC, Canada) according to the manufacturer's instructions and a previous report.<sup>(15)</sup> A single cell suspension (1  $\times$  10<sup>6</sup>) was mixed with activated ALDH substrate (StemCell Technologies Inc). Diethylaminobenzaldehyde (DEAB), which is a specific and irreversible inhibitor of ALDH, was used as a negative control. Finally, we isolated Aldefluor<sup>pos</sup> and Aldefluor<sup>neg</sup> populations under DEAB-negative conditions by cell sorter.

**Mammosphere formation assay.** Sample cells (1  $\times$  10<sup>4</sup>) were mixed in MammoCult medium (StemCell Technologies Inc) containing heparin and hydrocortisone and cultured for 7 days. Mammosphere (diameter  $\geq$ 100  $\mu$ m) forming efficiency (MSFE) was calculated as the number of mammospheres divided by the original number of cells seeded and indicated as percentage.

**Cell proliferation assay.** Cells (4  $\times$  10<sup>4</sup>) were plated on 35 mm dish and were cultured under normoxic conditions. Surviving cells were scored at 24-h intervals using the trypan-blue exclusion method.

**Wound healing assay.** Cells (1  $\times$  10<sup>5</sup>) were plated on six-well dishes. After cells reach confluency, a single scratch wound was created using a p10 micropipette into confluent cells. The migration distance ( $\mu$ m), at 0 and 24 h after wounding, was calculated using the ImageJ software program.

**Matrigel invasion assay.** Cells (4  $\times$  10<sup>4</sup>) in DMEM-high containing 0.1% FBS were seeded onto BD Matrigel Basement Membrane Matrix (BD Biosciences)-coated 8- $\mu$ m BD Falcon cell culture insert (BD Biosciences). DMEM containing 10% FBS was added to the lower compartments of each chamber, and cells were incubated for 24 h. After removal of the cells that remain in the top chamber, the top surface of each membrane was cleared of cells with a cotton swab. Cells that had penetrated to the bottom side of the membrane were then fixed in methanol, stained with a Diff-Quick Stain Set (Sysmex Corporation, Kobe, Japan), and counted.

**Animal studies.** Female C57BL/6J mice were purchased from Japan SLC, Inc (Shizuoka, Japan) and bred under SPF conditions with *ad libitum* access to food and water. All experimental procedures were approved by the University of Tsukuba Institute Animal Care and Use Committee. Sample cells (2  $\times$  10<sup>5</sup>) were injected into the tail vein and suspensions containing sample cells (5  $\times$  10<sup>6</sup>) in 100  $\mu$ L of Growth Factor Reduced BD Matrigel Matrix (BD Biosciences) were injected into the subcutaneous tissue. After 21 days, the mice were sacrificed by cervical dislocation and the primary tumors and lungs were analyzed. Immunosuppression was performed by Cyclosporin-A (Sigma-Aldrich, St. Louis, MO, USA) injection (20 mg/kg per day, i.p.).

**Immunohistochemistry.** The primary tumors and lungs were fixed with 4% paraformaldehyde (Wako Pure Chemical, Osaka, Japan). The sections of tumor samples were stained by Hematoxylin–Eosin. Four sections per sample were selected at random and the areas with tumor cell aggregation were measured. This aggregate area was then divided by the area of each tumor section to calculate mean tumor burden per tumor sample. The lung sections were stained by Hematoxylin–Eosin. Three sections per sample were selected at random and metastatic foci were counted in each section. Then, the number of metastases was divided by the area of the each lung section to calculate mean metastatic density per sample.

**Quantitative polymerase chain reaction (qPCR).** The cDNA samples were synthesized from total RNA (2  $\mu$ g) using a ReverTra Plus kit (TOYOBO, Osaka, Japan). The reaction mixtures for quantitative PCR were prepared using THUNDERBIRD SYBR qPCR Mix (TOYOBO). The data were calculated by the  $\Delta\Delta C_t$  method. The sequences of the primers used for qPCR are shown in Table 1.

**Western blotting analysis.** Proteins were subjected to Western blotting as previously described.<sup>(16,17)</sup> Anti-human HIF-1 $\alpha$  (1:2000; sc-10790, Santa Cruz Biotechnology, Santa Cruz, CA, USA),<sup>(18)</sup> anti-human HIF-2 $\alpha$  (1:3000; NB100-132, Novus Biologicals, Littleton, CO, USA),<sup>(19)</sup> anti-human Snail (1:2000;

**Table 1. Primers used for Quantitative polymerase chain reaction (qPCR)**

Human HIF-1 $\alpha$	Sense: 5'-TTACCGAATTGATGGGATATGAG-3' Antisense: 5'-TCATGATGAGTTTTGGTCAGATG-3'
Human HIF-2 $\alpha$	Sense: 5'-CTATGTGACTCGGATGGTCTTTC-3' Antisense: 5'-ATACCATTTTTGACCCTCATT-3'
Human E-cadherin	Sense: 5'-CTGGCCTCAGAAGACAGAAGAGAGACT-3' Antisense: 5'-CAGCGTGAGAGAAGAGAGTGTATGTGG-3'
Human Vimentin	Sense: 5'-CCGTTGAAGCTGCTAACTACCAAGAC-3' Antisense: 5'-GTGGGTATCAACCAGAGGGAGTGAAT-3'
Human Notch-1	Sense: 5'-CACTGTGGGCGGGTCC-3' Antisense: 5'-GTTGTATTGGTTCGGACCAT-3'
Human Jagged-1	Sense: 5'-CTATGATGAGGGGATGCT-3' Antisense: 5'-CGTCCATTGAGCACTGG-3'
Human TGF- $\beta$	Sense: 5'-AGAGCTCCGAGAAGCGGTACCTGAACCC-3' Antisense: 5'-GTTGATGTCCACTTGCACTGTGTTATCC-3'
Human Snail	Sense: 5'-AACTACAGCGAGCTGCAGGACTCTAA-3' Antisense: 5'-CCTTCCACTGCCTCATCTGACA-3'
Human Slug	Sense: 5'-CTCTCTTCCGGATACTCCTCATCT-3' Antisense: 5'-CCAGGCTCACATATTCCTTGTACAG-3'
Human ALDH1A1	Sense: 5'-GGAGTGTGAGCGGGCTAAGAAGTA-3' Antisense: 5'-CATTAGAGAACACTGTGGGCTGGAC-3'
Human VEGF	Sense: 5'-AGATGAGCTTCTACAGCAAC-3' Antisense: 5'-AGGACTTATACCGGATTTCTTG-3'
Human $\beta$ -actin	Sense: 5'-GTGCGTGACATTAAGGAGAAGCTGTGC-3' Antisense: 5'-GTAAGTGGCTCAGGAGGCAATGAT-3'

sc-28199, Santa Cruz Biotechnology), anti-human Slug (1:2000; sc-10436, Santa Cruz Biotechnology), anti-human Actin (1:2000; sc-1615, Santa Cruz Biotechnology) and anti-human Lamin B (1:3000; sc-6217, Santa Cruz Biotechnology) antibodies were used. Then, horse radish peroxidase (HRP)-conjugated secondary antibodies were incubated according to the manufacturer's instructions. The resultant signal was detected by chemiluminescence using the Immobilon Western Chemiluminescent HRP substrate (Merck Millipore, Billerica, MA, USA).

**Overexpression and shRNA treatment of HIF-1 $\alpha$  and siRNA treatment of HIF-2 $\alpha$ .** To overexpress HIF-1 $\alpha$ , cells were transfected with pEF-BOS-human HIF-1 $\alpha$  or pEF-BOS (control) using Lipofectamine LTX (Invitrogen). To suppress HIF-1 $\alpha$  expression, we used the MISSION shRNA lentiviral transduction system (TRCN000003810; Sigma-Aldrich).<sup>(20)</sup> GFP-expressing Aldefluor<sup>pos</sup> cells were established using MISSION TurboGFP Control Particle (SHC003V; Sigma-Aldrich) as control cells. And, to suppress HIF-2 $\alpha$  expression, cells were transfected with either HIF-2 $\alpha$  siRNA or negative control siRNA (Qiagen, Basel, Switzerland), using Lipofectamine LTX (Invitrogen).<sup>(21)</sup> All kits were used according to the manufacturer's instructions.

**Chromatin immunoprecipitation (ChIP) assay.** Sample cells ( $1.5 \times 10^7$ ) were fixed with 1% formaldehyde, then washed with phosphate-buffered saline (PBS) containing 1 mM protease inhibitor mixture (Roche Applied Science, Indianapolis, IN, USA). Nuclear extracts were prepared as described previously.<sup>(22)</sup> After fragmentation of DNA by sonication, the samples were incubated at 4°C with anti-human HIF-1 $\alpha$  (1:1000; NB100-105, Novus Biologicals) or anti-human HIF-2 $\alpha$

(1:1000; NB100-132, Novus Biologicals) antibodies. Normal rabbit IgG was used as a negative control. The reaction mixtures were incubated with protein A-agarose beads (Nacal Tesque, Kyoto, Japan) and were eluted with elution buffer (1% SDS, 0.1 M NaHCO<sub>3</sub>). DNA-protein complexes were denatured at 65°C. The ALDH1A1 HRE sequence was detected by PCR using Ex *Taq* polymerase (TAKARA BIO INC, Kyoto, Japan). The following primers were used: sense primer, 5'-ATCTCACCTTGAATTGTAGTTC-3' and antisense primer, 5'-TAATTGACTCACAGTTCAGCAT-3'.

**Statistical analysis.** The data are presented as the means  $\pm$  SD from three or more independent experiments. Sample means were compared using Student's *t*-test or an ANOVA, followed by Tukey's multiple comparison test. Calculations were executed by the GraphPad Prism software program (GraphPad Software Inc., La Jolla, CA, USA).

## Results

**Isolation and characterization of BCSC properties in primary breast cancer cells.** Previous studies have demonstrated that ALDH activity, reflected by Aldefluor<sup>pos</sup> status, is a good indicator of breast cancer cell lines that possess stem cell properties, such as self-renewal activity, tumorigenesis and metastasis.<sup>(5,23)</sup> After enrichment for a CD44<sup>+</sup>/CD24<sup>-</sup> population, we separated BC#1 on the basis of ALDH activity and cultivated it for further analyses (Fig. 1a).<sup>(14)</sup> Previously, we showed that BC#1 is CK5/6<sup>+</sup>, CK8<sup>+</sup>, ER<sup>+</sup>, PgR<sup>+</sup>, HER2<sup>-</sup>.<sup>(14)</sup> In order to validate the phenotype of BC#1 in further detail, we examined the expression of CK14 (a breast epithelial marker) and Vimentin (a fibroblast marker), and showed that BC#1 is CK14<sup>+</sup> and Vimentin<sup>-</sup>, suggesting that BC#1 is consisted of breast cancer cells (data not shown). With regard to cellular morphology, the CD44<sup>+</sup>/CD24<sup>-</sup>/Aldefluor<sup>neg</sup> population showed an epithelial-like morphology whereas the CD44<sup>+</sup>/CD24<sup>-</sup>/Aldefluor<sup>pos</sup> population showed both epithelial-like and spindle-shaped morphology (Fig. 1b). The Aldefluor<sup>pos</sup> cells proliferated more rapidly compared with the Aldefluor<sup>neg</sup> cells as previously reported (Fig. 1c).<sup>(23)</sup> The mammosphere assay showed that the Aldefluor<sup>pos</sup> cells had a higher mean MSFE than the Aldefluor<sup>neg</sup> cells in both the primary and secondary assays (Fig. 1d). And the wound healing assay showed that the migration distance of the Aldefluor<sup>pos</sup> cells was greater than that of the Aldefluor<sup>neg</sup> cells (Fig. 1e). Furthermore, the matrigel invasion assay showed that the number of passed cells per field of Aldefluor<sup>pos</sup> cells was more than that of the Aldefluor<sup>neg</sup> cells (Fig. 1f). These findings fit with previous reports that deem it likely that the Aldefluor<sup>pos</sup> cell population may be enriched in cancer stem/progenitor cells compared with the Aldefluor<sup>neg</sup> cell population.<sup>(23,24)</sup>

The number of pulmonary metastases was significantly increased in the mice injected with Aldefluor<sup>pos</sup> cells compared with Aldefluor<sup>neg</sup> cells (Fig. 1g). The Aldefluor<sup>pos</sup> cell-derived tumors were larger than those derived from Aldefluor<sup>neg</sup> cells and there was a significant difference in the tumor burden (Fig. 1h). Taken together, these data indicate that Aldefluor<sup>pos</sup> BC#1 cells have increased stem cell properties, compared with Aldefluor<sup>neg</sup> BC#1 cells, as previously reported.<sup>(4,25)</sup>

**Analysis of the relationship between hypoxia and BCSCs.** Previous reports demonstrated that activated HIFs in BCCs can promote self-renewal, survival, tumorigenicity, invasiveness and metastasis.<sup>(26-28)</sup> Indeed, the HIF-1 $\alpha$  expression was significantly increased in Aldefluor<sup>pos</sup> cells compared with Aldefluor<sup>neg</sup> cells under hypoxic conditions (Fig. 2a,b). In contrast,



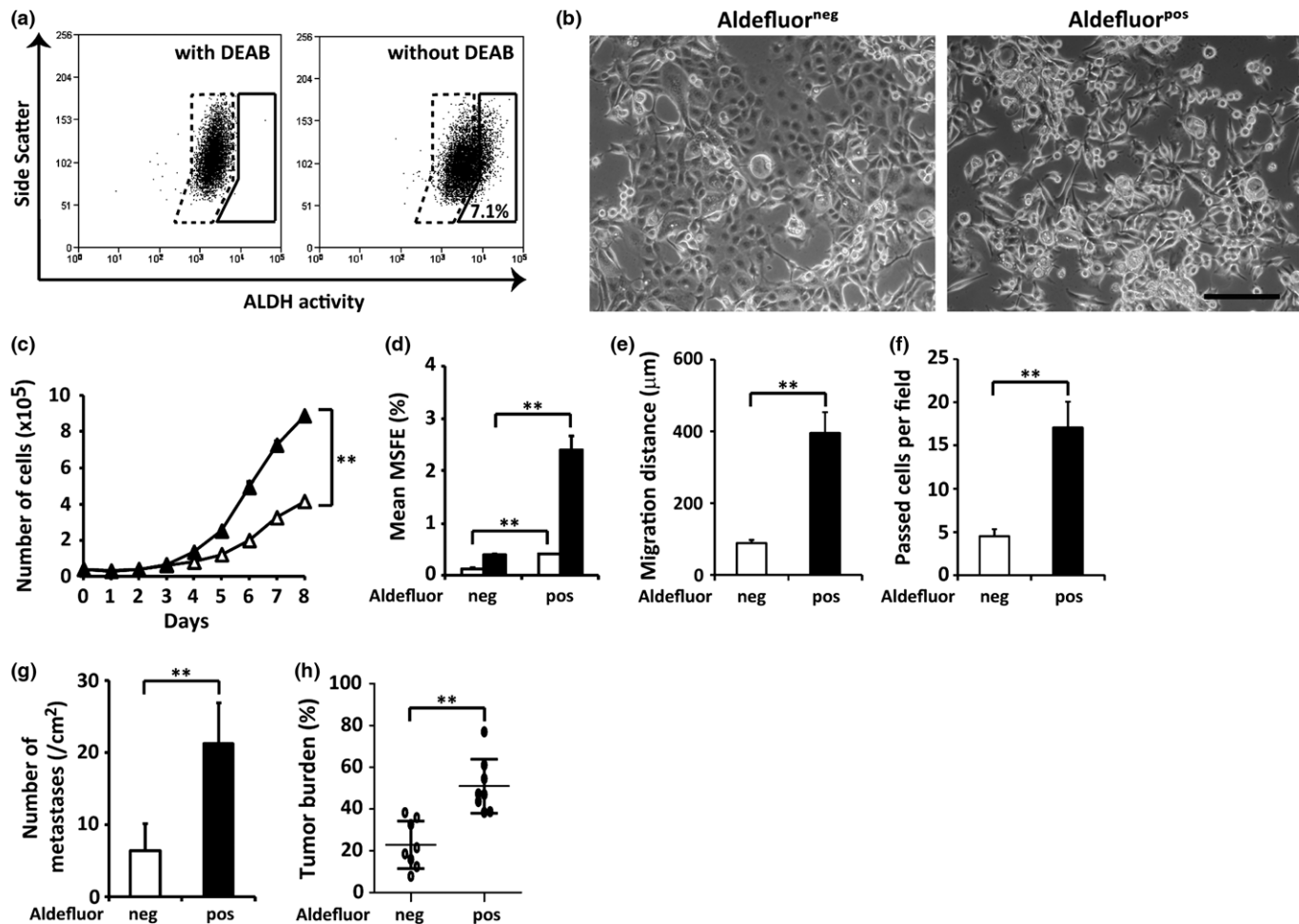


**Fig. 1.** The characteristics of Aldefluor<sup>neg</sup> and Aldefluor<sup>pos</sup> cells in breast cancer cells (BCCs). (a) The flow cytometric analyses of the ALDH activity in CD44<sup>+</sup>/CD24<sup>-/low</sup> cells (BC#1). Isolated Aldefluor<sup>pos</sup> BC#1 in the solid line and Aldefluor<sup>neg</sup> BC#1 in the dotted line. (b) The morphology of Aldefluor<sup>neg</sup> and Aldefluor<sup>pos</sup> BC#1. Scale bar = 200 μm. (c) The proliferation of Aldefluor<sup>neg</sup> (white triangles) and Aldefluor<sup>pos</sup> (black triangles) BC#1 under normoxic conditions. (d) The mean mammosphere forming efficiency (MSFE) of the Aldefluor<sup>neg</sup> and Aldefluor<sup>pos</sup> BC#1 cultures determined by the mammosphere formation assay. Primary mammospheres (white bar), secondary mammospheres (black bar). (e) The migration distance of Aldefluor<sup>neg</sup> and Aldefluor<sup>pos</sup> BC#1 was determined by the wound healing assay. (f) The migrated cells per field of Aldefluor<sup>neg</sup> and Aldefluor<sup>pos</sup> BC#1 was determined by the matrigel invasion assay. (g) The number of hematogenous metastases in the lungs of mice that received Aldefluor<sup>neg</sup> or Aldefluor<sup>pos</sup> BC#1 by tail vein injection. (h) Tumor burden size derived from Aldefluor<sup>neg</sup> or Aldefluor<sup>pos</sup> BC#1 by subcutaneous transplantation. The data are presented as the means ± SD from three independent experiments. \*\**P* < 0.01 by Student's *t*-test or ANOVA with Tukey's multiple comparison test.

HIF-2 $\alpha$  was expressed at a similar level under both normoxic and hypoxic conditions. In addition, there was no significant difference in the HIF-2 $\alpha$  expression between the Aldefluor<sup>pos</sup> cells and Aldefluor<sup>neg</sup> cells (Figs. 2a,b,S1a). We then investigated whether knockdown of HIF-2 $\alpha$  expression would affect the stem cell properties of Aldefluor<sup>pos</sup> cells and Aldefluor<sup>neg</sup> cells. The HIF-2 $\alpha$  expression was significantly suppressed in both cells transfected with HIF-2 $\alpha$  siRNA (siHIF-2 $\alpha$ ) compared with the control (siControl) and HIF-1 $\alpha$  expression was unaffected in the siHIF-2 $\alpha$  and the siControl (Fig. 2c,d). Knockdown of HIF-2 $\alpha$  expression in both cell groups led to an increased dead cell number (Fig. 2e), suggesting that HIF-2 $\alpha$  may have a role in maintaining survival of both Aldefluor<sup>pos</sup> and Aldefluor<sup>neg</sup> cells, as previously reported.<sup>(29)</sup>

Previous reports demonstrated that HIF-1 $\alpha$  triggers the EMT by decreasing E-cadherin expression and increasing Vimentin expression.<sup>(30,31)</sup> The Vimentin mRNA level was increased, whereas the E-cadherin mRNA level was decreased, in Aldefluor<sup>pos</sup> cells compared with Aldefluor<sup>neg</sup> cells under hypoxic

conditions (Fig. 2f). Similarly, the FACS analysis showed that the frequency of E-cadherin-positive cells was markedly reduced, but the frequency of Vimentin-positive cells was significantly elevated in the Aldefluor<sup>pos</sup> cells (Fig. 2g). We could detect the change of these EMT markers at the protein level in the Aldefluor<sup>pos</sup> cells and considered that the protein levels reflect cellular milieu more precisely than the mRNA level.

Importantly, previous studies have shown that HIF-1 $\alpha$  activates several signaling pathways, such as the Notch and TGF- $\beta$  signaling pathways, which in turn induce the expression of EMT-associated transcription factors, such as Snail and Slug.<sup>(11,32)</sup> We found the expression levels of Notch-1, Jagged-1 and TGF- $\beta$  were significantly increased in Aldefluor<sup>pos</sup> cells compared with Aldefluor<sup>neg</sup> cells under hypoxic conditions (Fig. 2h). In addition, the protein expression of Snail and Slug were significantly upregulated in Aldefluor<sup>pos</sup> cells compared with the Aldefluor<sup>neg</sup> cells under both normoxic and hypoxic conditions (Fig. 2i,j). Under normoxic conditions, HIF-1 $\alpha$  protein was slightly increased in Aldefluor<sup>pos</sup> cells compared with

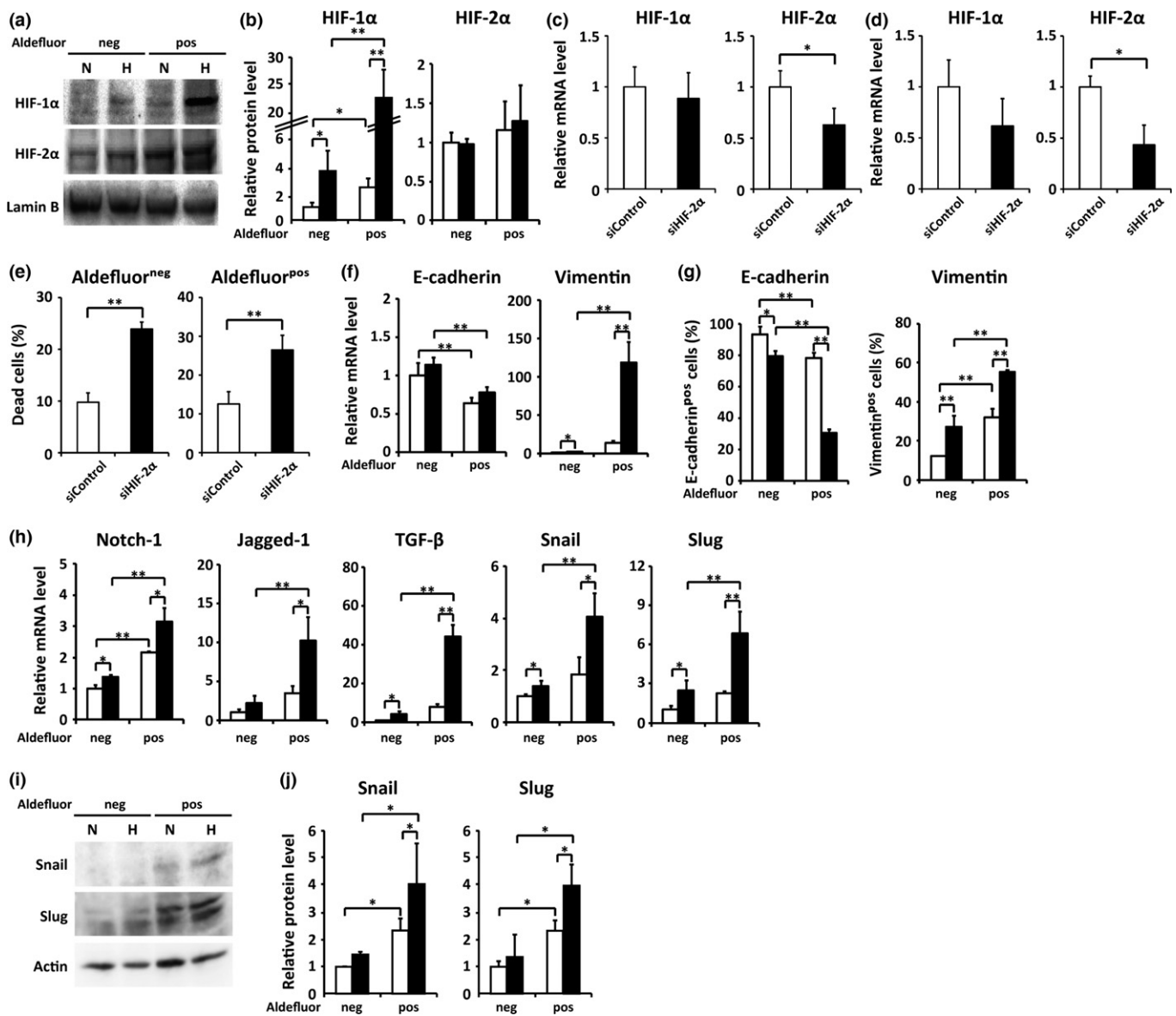


**Fig. 2.** Hypoxic response of Aldefluor<sup>neg</sup> and Aldefluor<sup>pos</sup> BC#1. (a), (b) The protein expression of hypoxia-inducible factors (HIFs) (HIF-1 $\alpha$  and HIF-2 $\alpha$ ) in BC#1 cultured under normoxic (20% O<sub>2</sub>, N: white bar) or hypoxic (1% O<sub>2</sub>, H: black bar) conditions. (c), (d) The mRNA expression of HIF-1 $\alpha$  and HIF-2 $\alpha$  in Aldefluor<sup>neg</sup> (c) and Aldefluor<sup>pos</sup> cells (d) transfected with HIF-2 $\alpha$  siRNA or Control siRNA under normoxic conditions. (e) The percentage of dead cells in Aldefluor<sup>neg</sup> and Aldefluor<sup>pos</sup> cells after transfection with HIF-2 $\alpha$  siRNA under normoxic conditions. (f) The mRNA expression of E-cadherin and Vimentin in BC#1 cultured under normoxic (white bar) or hypoxic (black bar) conditions. (g) The protein expression of E-cadherin and Vimentin in BC#1 cultured under normoxic (white bar) or hypoxic (black bar) conditions for 24 h, as determined by flow cytometry. (h) The mRNA expression of each factor in BC#1 cultured under normoxic (white bar) or hypoxic (black bar) conditions. (i), (j) The protein expression of Snail and Slug in BC#1 cultured under normoxic (20% O<sub>2</sub>, N: white bar) or hypoxic (1% O<sub>2</sub>, H: black bar) conditions as determined by Western blotting analysis. The data are presented as the means  $\pm$  SD analysis from three independent experiments. \* $P$  < 0.05; \*\* $P$  < 0.01 by Student's  $t$ -test or ANOVA with Tukey's multiple comparison test.

Aldefluor<sup>neg</sup> cells (Fig. 2b). Thus, these data suggested that HIF-1 $\alpha$  might upregulate Snail and Slug expression in Aldefluor<sup>pos</sup> cells under normoxic conditions as previously reported.<sup>(33–35)</sup>

**Knockdown of HIF-1 $\alpha$  expression in Aldefluor<sup>pos</sup> cells reduced their stem cell properties.** We then asked whether knockdown of HIF-1 $\alpha$  expression would affect the BCSC properties of Aldefluor<sup>pos</sup> cells. The HIF-1 $\alpha$  expression was markedly repressed in Aldefluor<sup>pos</sup> cells that were transfected with HIF-1 $\alpha$  shRNA (Aldefluor<sup>pos</sup>-shHIF-1 $\alpha$ ) compared with the control (Aldefluor<sup>pos</sup>-shGFP), whereas there was no significant

difference in the HIF-2 $\alpha$  expression in the Aldefluor<sup>pos</sup>-shHIF-1 $\alpha$  and the control (Figs. 3a,b,S1b). Knocking down HIF-1 $\alpha$  expression in Aldefluor<sup>pos</sup> cells led to a decreased population of spindle-shaped cells (data not shown), and knockdown of HIF-1 $\alpha$  in the Aldefluor<sup>pos</sup> cells affected the number of cells on day 8, suggesting that HIF-1 $\alpha$  knockdown may inhibit the proliferation of Aldefluor<sup>pos</sup> cells (Fig. 3c). The mammosphere formation assay demonstrated that Aldefluor<sup>pos</sup>-shHIF-1 $\alpha$  cells showed a decreased mean MSFE compared with the control cells (Fig. 3d). We examined the mRNA expression of stem regulator genes; OCT4 and Nanog, and found these expression

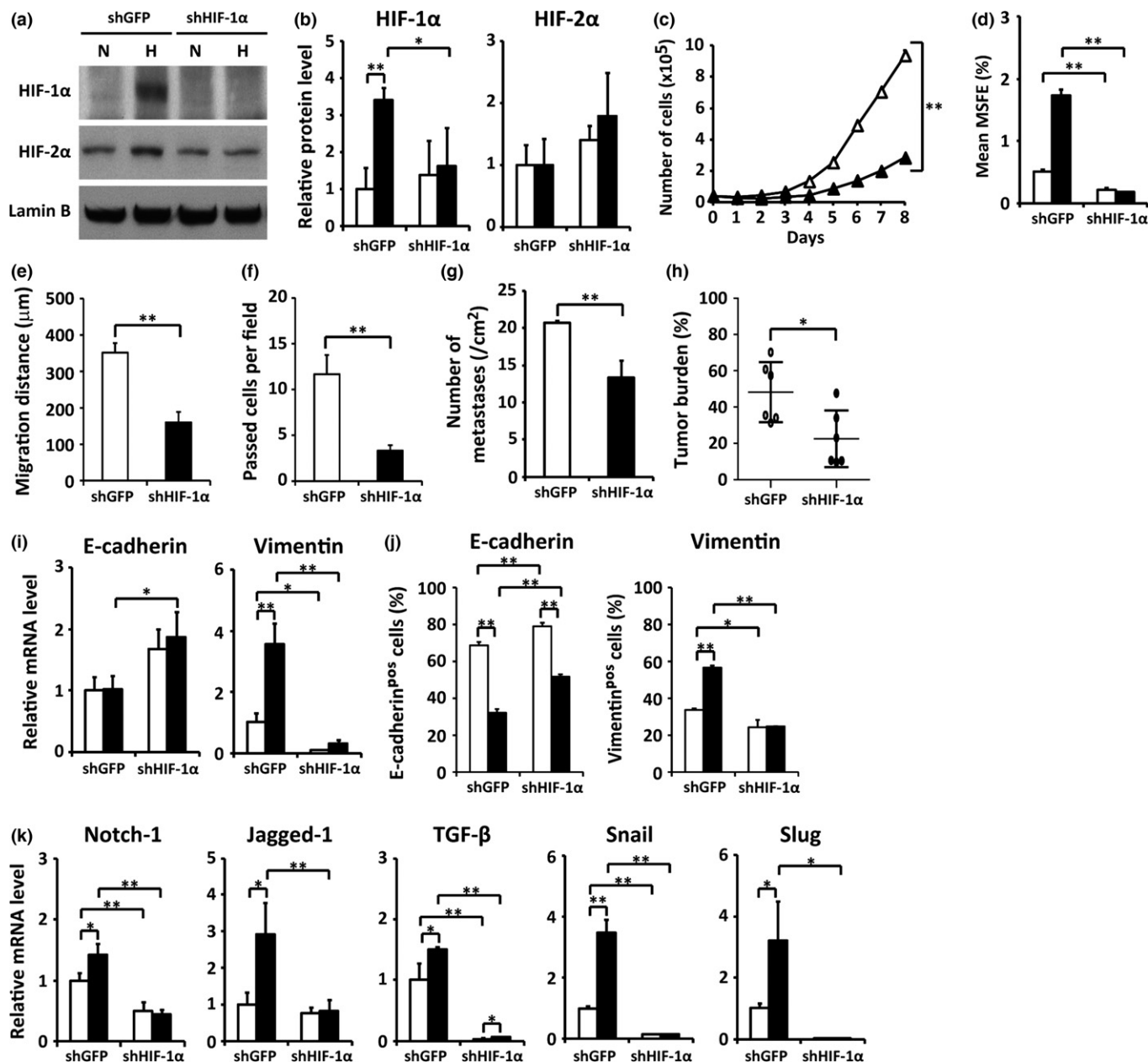


**Fig. 3.** Reduction of stem cell properties in Aldefluor<sup>POS</sup> BC#1 by hypoxia-inducible factor (HIF)-1 $\alpha$  knockdown. (a), (b) The protein expression of HIF-1 $\alpha$  and HIF-2 $\alpha$  in Aldefluor<sup>POS</sup>-shGFP or Aldefluor<sup>POS</sup>-shHIF-1 $\alpha$  BC#1 cells cultured under normoxic (N: white bar) or hypoxic (H: black bar) conditions. (c) The cell proliferation activities of Aldefluor<sup>POS</sup>-shGFP (white triangles) and Aldefluor<sup>POS</sup>-shHIF-1 $\alpha$  (black triangles) cells under normoxic conditions. (d) The mean mammosphere forming efficiency (MSFE) for the first mammospheres (white bar) and secondary mammospheres (black bar). (e) The migration activities. (f) The cell invasion activities. (g) The number of hematogenous metastases in the lungs. (h) The size of tumor burden derived from Aldefluor<sup>POS</sup>-shHIF-1 $\alpha$  cells. (i) The mRNA expression of E-cadherin and Vimentin in cells cultured under normoxic (white bar) or hypoxic (black bar) conditions. (j) The protein expression of E-cadherin and Vimentin in cells cultured under normoxic (white bar) or hypoxic (black bar) conditions for 24 h, was determined by flow cytometry. (k) The mRNA expression of each factor in cells cultured under normoxic (white bar) or hypoxic (black bar) conditions. The data are presented as the means  $\pm$  SD from three independent experiments. \* $P$  < 0.05; \*\* $P$  < 0.01 by Student's  $t$ -test or ANOVA with Tukey's multiple comparison test.

levels were significantly decreased, suggesting that knockdown of HIF-1 $\alpha$  suppresses the maintenance of stemness of Aldefluor<sup>POS</sup> cells (data not shown). Furthermore, the wound healing assay demonstrated that the migration distance of Aldefluor<sup>POS</sup>-shHIF-1 $\alpha$  cells was smaller than that of the control cells (Fig. 3e). And the matrigel invasion assay showed that Aldefluor<sup>POS</sup>-shHIF-1 $\alpha$  cells showed reduced number of invasive cells per field compared with the control cells (Fig. 3f).

We then examined the number of pulmonary metastases, and found that the number of foci was significantly decreased by the injection of Aldefluor<sup>POS</sup>-shHIF-1 $\alpha$  cells compared with the control (Fig. 3g). An *in vivo* subcutaneous transplantation assay also demonstrated that tumors derived from Aldefluor<sup>POS</sup>-shHIF-1 $\alpha$  cells showed a decreased weight and volume compared with the control (data not shown). The histological analyses of tumor sections by Hematoxylin–Eosin staining

clearly showed a decreased tumor burden in the mice bearing Aldefluor<sup>pos</sup>-shHIF-1 $\alpha$  cells compared with the control (Fig. 3h).

In order to determine whether knockdown of HIF-1 $\alpha$  affected the expression of EMT-related genes, we examined the E-cadherin and Vimentin expression in Aldefluor<sup>pos</sup>-shHIF-1 $\alpha$  cells. Increased expression of E-cadherin and decreased expression of Vimentin was observed in the HIF-1 $\alpha$  knock-down Aldefluor<sup>pos</sup> cells under hypoxic conditions (Fig. 3i). Similarly, the FACS analysis showed that the frequency of E-cadherin-positive cells was markedly increased, but the frequency of Vimentin-positive cells was significantly decreased in the HIF-1 $\alpha$  knockdown Aldefluor<sup>pos</sup> cells (Fig. 3j). Furthermore, we found a significant decrease in the expression of Notch-1, Jagged-1, TGF- $\beta$ , Snail and Slug in the Aldefluor<sup>pos</sup>-shHIF-1 $\alpha$  cells compared with control cells under hypoxic conditions (Fig. 3k). In addition, we examined whether Notch signaling blocks Hypoxia-induced EMT in Aldefluor<sup>pos</sup> cells using a Notch inhibitor (DAPT), and showed the expression of EMT-related genes, in Aldefluor<sup>pos</sup> cells treated with DAPT, were significantly increased under the hypoxic conditions (Fig. S2). However, the expression level of the EMT-related genes; Snail and Slug in Aldefluor<sup>pos</sup> cells treated with DAPT was lower compared with the control cells. These results indicated that a Notch inhibitor could not block total hypoxia-induced EMT, suggesting Notch signaling-induced EMT is partially but not fully dependent on hypoxia. Collectively, these results suggest that HIF-1 $\alpha$  is highly associated with the stem cell properties of Aldefluor<sup>pos</sup> cells by promoting the EMT process.

**HIF-1 $\alpha$  overexpression induced the elevated expression of Snail and Slug mRNA in Aldefluor<sup>neg</sup> cells.** We then transfected HIF-1 $\alpha$  into Aldefluor<sup>neg</sup> cells to determine whether HIF-1 $\alpha$  overexpression induces Snail or Slug in BCCs. The HIF-1 $\alpha$  protein was constitutively expressed even under normoxic conditions

in the HIF-1 $\alpha$ -transfected Aldefluor<sup>neg</sup> cells (Fig. 4a,b). The Aldefluor<sup>neg</sup>-pEF-BOS-HIF-1 $\alpha$  cells showed epithelial morphology and seemed to contain more spindle-shaped cells than the control (Aldefluor<sup>neg</sup>-pEF-BOS cells) (data not shown). We also found decreased expression of E-cadherin and increased expression of Vimentin in the Aldefluor<sup>neg</sup>-pEF-BOS-HIF-1 $\alpha$  cells compared with the control (Fig. 4c). Similarly, the FACS analysis showed that the frequency of E-cadherin-positive cells was markedly decreased, but the frequency of Vimentin-positive cells was significantly increased in the Aldefluor<sup>neg</sup>-pEF-BOS-HIF-1 $\alpha$  cells (Fig. 4d). There were no significant differences in Notch-1, Jagged-1 or TGF- $\beta$  expression whereas the expression levels of Snail and Slug were significantly increased in the Aldefluor<sup>neg</sup>-pEF-BOS-HIF-1 $\alpha$  cells (Fig. 4e). These results indicate that HIF-1 $\alpha$  overexpression was involved in triggering the EMT process, which occurred through the repression of E-cadherin due to the induction of Snail and Slug expression in the Aldefluor<sup>neg</sup> cells.

The number of pulmonary metastases was markedly increased in mice injected with Aldefluor<sup>neg</sup>-pEF-BOS-HIF-1 $\alpha$  cells compared with the control (Fig. 4f). The tumor burden of the mice injected with Aldefluor<sup>neg</sup>-pEF-BOS-HIF-1 $\alpha$  cells was significantly higher than the control (Fig. 4g). Taken together, these results indicate that HIF-1 $\alpha$  affects the phenotypic change of BCSC population in regards to tumorigenesis and metastasis.

**Aldefluor<sup>neg</sup> cells were altered to Aldefluor<sup>pos</sup> cells in a process directly regulated by HIF-1 $\alpha$ .** It has been reported that the mRNA level of ALDH1A1 positively correlates with the ALDH activity in BCSCs.<sup>(36)</sup> The expression of ALDH1A1 was significantly increased in the Aldefluor<sup>neg</sup>-pEF-BOS-HIF-1 $\alpha$  cells and the expression of ALDH1A1 was significantly decreased in the Aldefluor<sup>pos</sup>-shHIF-1 $\alpha$  cells (Fig. 5a). Indeed, the ALDH activity in the Aldefluor<sup>pos</sup>-shHIF-1 $\alpha$  cells was markedly decreased compared with the control Aldefluor<sup>pos</sup>

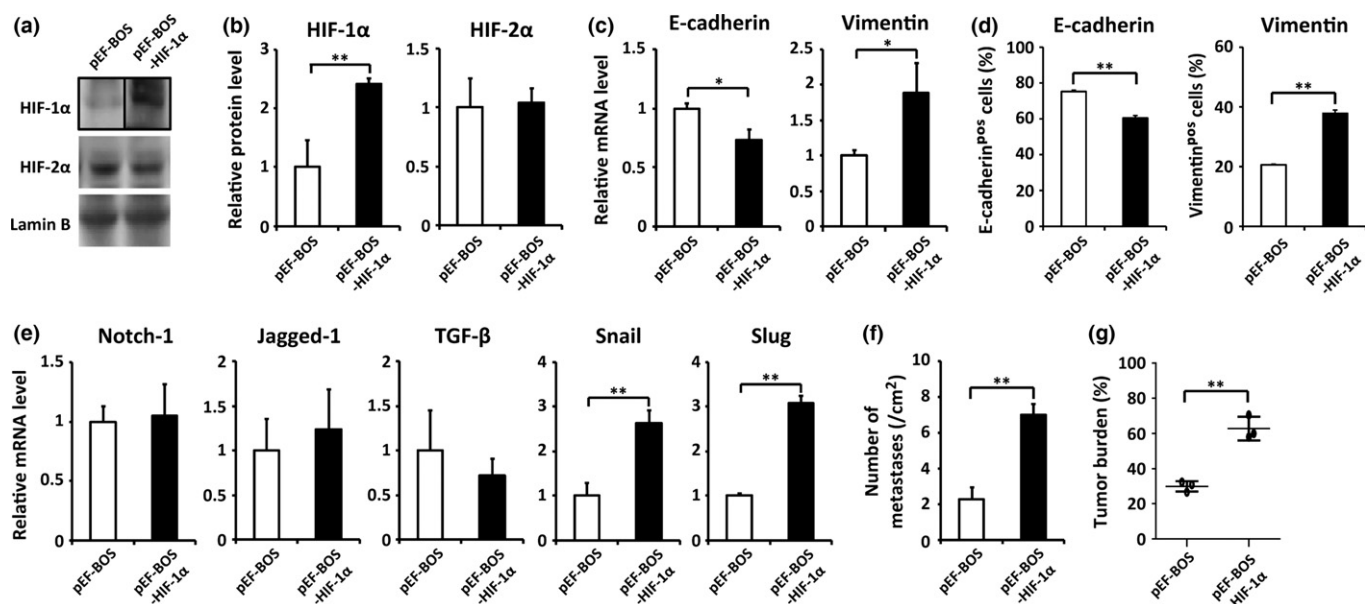


**Fig. 4.** The stem cell properties of Aldefluor<sup>neg</sup> BC#1 cells were increased by hypoxia-inducible factor (HIF)-1 $\alpha$ -overexpression. (a), (b) The protein expression of HIFs (HIF-1 $\alpha$  and HIF-2 $\alpha$ ) in Aldefluor<sup>neg</sup>-pEF-BOS (pEF-BOS) and Aldefluor<sup>neg</sup>-pEF-BOS-HIF-1 $\alpha$  (pEF-BOS-HIF-1 $\alpha$ ) BC#1 was examined in cells cultured under normoxic conditions. (c) The mRNA expression of E-cadherin and Vimentin in cells cultured under normoxic conditions. (d) The protein expression of E-cadherin and Vimentin in cells cultured under normoxic conditions. (e) The mRNA expression of each factor in cells cultured under normoxic conditions. (f) The number of hematogenous metastases in the lungs. (g) Tumor burden size derived from pEF-BOS-HIF-1 $\alpha$  BC#1. The data are presented as the means  $\pm$  SD from three independent experiments. \* $P$  < 0.05; \*\* $P$  < 0.01 by Student's  $t$ -test.



cells. On the other hand, the ALDH activity in the Aldefluor<sup>neg</sup>-pEF-BOS-HIF-1 $\alpha$  cells was markedly increased compared with the control Aldefluor<sup>neg</sup>-pEF-BOS cells (Fig. 5b). These results indicate that HIF-1 $\alpha$  expression is highly associated with the increase in ALDH activity via a direct and/or indirect manner.

In order to address specificity in HIF-1 $\alpha$  or HIF-2 $\alpha$  binding to the ALDH1A1 promoter, we performed a ChIP assay using Aldefluor<sup>pos</sup> and Aldefluor<sup>neg</sup> cells. A direct association of HIF-1 $\alpha$  with the ALDH1A1 promoter was observed in Aldefluor<sup>pos</sup> cells under normoxic and hypoxic conditions, whereas HIF-1 $\alpha$  bound to the ALDH1A1 promoter in Aldefluor<sup>neg</sup> cells under hypoxic conditions (Fig. 5c). On the other hand, HIF-2 $\alpha$  could not bind to the ALDH1A1 promoter in both Aldefluor<sup>pos</sup> and Aldefluor<sup>neg</sup> cells.

Remarkably, we found that exposure to hypoxic stimuli for over 72 h significantly increased the frequency of Aldefluor<sup>pos</sup> cells in the Aldefluor<sup>neg</sup> population and led to a slight increase in total Aldefluor<sup>pos</sup> cells (Fig. 5d), suggesting that the ALDH activity in BC#1 may be regulated by HIF-1 $\alpha$  in some part. In fact, the phenotypic change from Aldefluor<sup>neg</sup> cells to Aldefluor<sup>pos</sup> cells was observed after 72 h under hypoxic conditions. We could detect similar phenomena using other breast cancer cell lines; MCF7 (HER2-negative) and SK-BR-3 (HER2-positive), suggesting that the alteration of Aldefluor<sup>pos</sup> cells derived from Aldefluor<sup>neg</sup> cells might not be HER2-negative specific (Fig. S3). In addition, we found that those altered Aldefluor<sup>pos</sup> cells derived from Aldefluor<sup>neg</sup> cells had increased expression of angiogenesis-related mRNA rather than EMT master genes (Fig. 5e).

Furthermore, the number of pulmonary metastases was significantly increased when hypoxia-induced Aldefluor<sup>pos</sup> cells derived from Aldefluor<sup>neg</sup> populations were injected and the number of metastatic foci caused by those population reached a similar level as native Aldefluor<sup>pos</sup> cells (Fig. 5f). In addition, the tumor burden of the mice injected with these derived cells was significantly higher than those of the mice injected with Aldefluor<sup>neg</sup> cells and was similar in level to Aldefluor<sup>pos</sup> cells (Fig. 5g).

Next we examined how ALDH1A1 contributes to the alteration process from Aldefluor<sup>pos</sup> to Aldefluor<sup>neg</sup> cells under hypoxic conditions. We treated Aldefluor<sup>pos</sup> cells with an ALDH1A1 inhibitor. It was clearly shown that an ALDH1A1 inhibitor suppress the increase of Aldefluor<sup>pos</sup> cells derived from Aldefluor<sup>neg</sup> cells under hypoxic conditions, suggesting that ALDH expression is associated with the alteration of Aldefluor<sup>pos</sup> cells from Aldefluor<sup>neg</sup> cells (data not shown).

Taken together, these results suggest that under hypoxic conditions, generation of Aldefluor<sup>pos</sup> cells might be induced by a different mechanism and those phenotypically altered Aldefluor<sup>pos</sup> populations might be highly associated with angiogenesis in tumor development (Fig. 5h).

## Discussion

Previous studies have suggested that traditional cancer treatments are effective for cancer reduction but fail to eliminate the CSCs that result in metastasis and recurrence. In order to examine the characteristics of BCSCs, we isolated primary cultured human breast cancer cells, BC#1, from a pleural effusion of breast cancer and selected CD44<sup>+</sup>/CD24<sup>-</sup> cells from which Aldefluor<sup>pos</sup> or Aldefluor<sup>neg</sup> populations were derived. The CD44<sup>+</sup>/CD24<sup>-</sup>/Aldefluor<sup>pos</sup> cells possessed more BCSC properties than the CD44<sup>+</sup>/CD24<sup>-</sup>/Aldefluor<sup>neg</sup> cells. Charafe-

Jauffret *et al.*<sup>(5)</sup> found that 23 out of 33 breast cancer cell lines examined contained an Aldefluor-positive population that displayed stem cell properties *in vivo* as well as in *in vitro* assays. These results suggested that high ALDH activity is a useful stem cell marker for primary cells as established BCC lines.<sup>(4,37)</sup>

In the case of tumorigenesis several HIF target genes play critical roles.<sup>(38)</sup> Among these HIF targeting genes, angiogenic factors, such as vascular endothelial growth factor (VEGF), are well-known target genes that play important roles in cancer development. Of critical importance is the previous report that HIF-1 $\alpha$  protein was not detected in specimens from normal breast tissue or ductal hyperplasia but was detected in the majority of samples of ductal carcinoma *in situ* and invasive cancer specimens.<sup>(27)</sup> Recently, several anti-angiogenic drugs have been developed; however, a previous study demonstrated that treatment with anti-angiogenic agents, including sunitinib and bevacizumab, actually increased the population of BCSCs and promoted tumorigenesis through HIF-1 $\alpha$  activation.<sup>(36)</sup> In this study, we showed that HIF-1 $\alpha$ , rather than HIF-2 $\alpha$ , is the key molecule associated with the maintenance of the stem cell properties of BCSCs. In addition, we found that HIF-1 $\alpha$  expression, but not HIF-2 $\alpha$  expression, was markedly increased in Aldefluor<sup>pos</sup> cells compared with Aldefluor<sup>neg</sup> cells in primary culture of BCCs and that HIF-2 $\alpha$  is associated with the survival of both Aldefluor<sup>pos</sup> and Aldefluor<sup>neg</sup> cells in the culture. Collectively, it is suggested that HIF-1 $\alpha$  expression is an important phenotype maintenance factor for BCSCs and that HIF-2 $\alpha$  is important for cellular survival.<sup>(3)</sup>

Hypoxic stimuli also exert physiological effects that can induce the EMT in tumors through multiple distinct mechanisms, including the upregulation of HIF-1 $\alpha$ , or activation of the Notch or NF- $\kappa$ B pathways.<sup>(33,39)</sup> Recent studies have demonstrated that HIF-1 $\alpha$ -mediated EMT is linked to CSC characteristics in brain cancer.<sup>(40)</sup> In the present study, we found that the both mRNA and protein levels of EMT trigger genes, Snail and Slug, were markedly increased in Aldefluor<sup>pos</sup> cells compared with Aldefluor<sup>neg</sup> cells in primary cultured BCCs. Indeed, knockdown of HIF-1 $\alpha$  expression in the Aldefluor<sup>pos</sup> cells reduced their capacity for self-renewal and their proliferation potential *in vitro*, as well as their tumorigenesis and metastasis *in vivo*, through inhibiting the EMT process via decreases in expression levels of Snail and Slug. We also found that HIF-1 $\alpha$  overexpression in Aldefluor<sup>neg</sup> cells increased the expression of Snail and Slug, thereby repressing the expression of E-cadherin and inducing the expression of Vimentin.

Importantly, we found that HIF-1 $\alpha$  directly induced ALDH1A1 mRNA expression, resulting in the production of Aldefluor<sup>pos</sup> cells derived from Aldefluor<sup>neg</sup> population by HIF-1 $\alpha$ . Ginestier and colleagues proposed that ALDH1 expression in a subset of tumors may reflect the transformation of ALDH-positive stem or early progenitors. By contrast, ALDH1-negative tumors may be generated by the transformation of ALDH1-negative progenitor cells.<sup>(4)</sup> In this study, we could identify the generation of Aldefluor<sup>pos</sup> cells from some part of the Aldefluor<sup>neg</sup> population under direct regulation by HIF-1 $\alpha$ . This result suggests that a small subset of the stem cell population would possess the reverse ability in terms of the expression of ALDH1A1. If this hypothesis is correct, it will be important to investigate the mechanism by which the ALDH expression is switched among CSCs and progenitor populations. Further analyses would be necessary to clarify this possible mechanism.



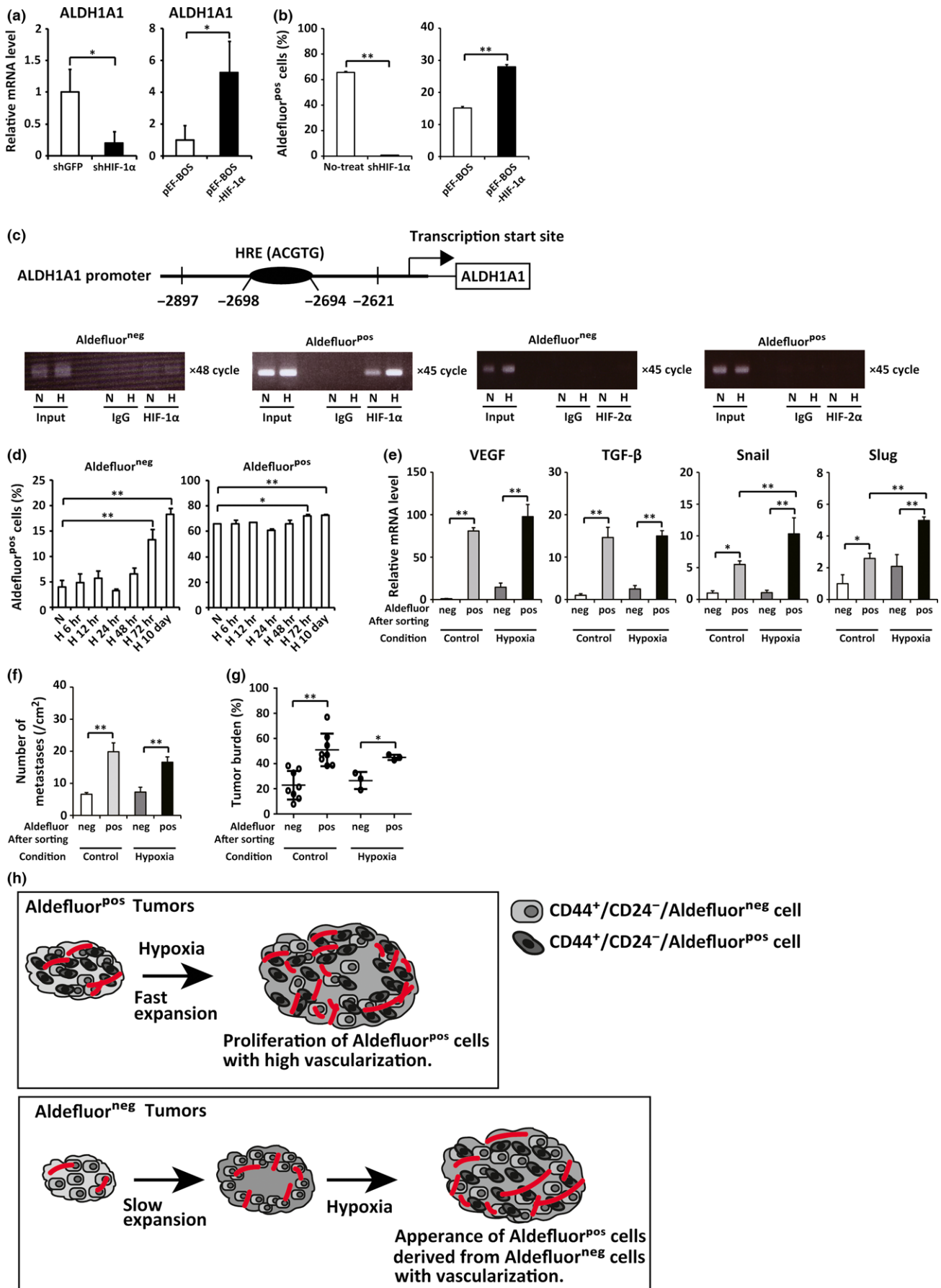


**Fig. 5.** The alternation of aldehyde dehydrogenase (ALDH) activity from Aldefluor<sup>neg</sup> cells to Aldefluor<sup>pos</sup> cells by hypoxia-inducible factor (HIF)-1 $\alpha$ . (a) The mRNA expression of ALDH1A1 (right: Aldefluor<sup>neg</sup>-pEF-BOS versus Aldefluor<sup>neg</sup>-pEF-BOS-HIF-1 $\alpha$ ; left: Aldefluor<sup>pos</sup>-shGFP versus Aldefluor<sup>pos</sup>-shHIF-1 $\alpha$ ) in BC#1 cultured under normoxic conditions was determined by qPCR. (b) The ALDH activity (right: Aldefluor<sup>neg</sup>-pEF-BOS versus Aldefluor<sup>neg</sup>-pEF-BOS-HIF-1 $\alpha$ ; left: untreated Aldefluor<sup>pos</sup> versus Aldefluor<sup>pos</sup>-shHIF-1 $\alpha$ ) in BC#1 cultured under normoxic conditions was determined by qPCR. (c) The location of the HRE in the ALDH1A1 promoter region (upper). The binding of HIF-1 $\alpha$  and HIF-2 $\alpha$  to the ALDH1A1 promoter's putative HRE was determined by the ChIP assay under normoxic (N) or hypoxic (H) conditions for 6 h (lower). Input: internal control; IgG: negative control. (d) The results of the flow cytometric analyses of the ALDH activity in Aldefluor<sup>pos</sup> and Aldefluor<sup>neg</sup> BC#1 cultured under normoxic (N) or hypoxic (H) conditions. (e) The mRNA expression of each factor in the Aldefluor<sup>pos</sup> (black bar) and Aldefluor<sup>neg</sup> (deep gray bar) cells after a 72-h exposure to hypoxia compared to the Aldefluor<sup>neg</sup> cells (white bar) and Aldefluor<sup>pos</sup> (light gray bar) before exposure (control). (f) The number of hematogenous metastases in the lungs. (g) Tumor burden size derived from the Aldefluor<sup>pos</sup> (black bar) or Aldefluor<sup>neg</sup> (deep gray bar) cells after a 72-h exposure to hypoxia compared to the Aldefluor<sup>neg</sup> cells (white bar) and Aldefluor<sup>pos</sup> (light gray bar) before exposure (control). (h) A schematic diagram summarizing the study. Aldefluor<sup>pos</sup> cells with characteristics of breast cancer stem cells (BCSCs) rapidly proliferate and form large tumors whereas Aldefluor<sup>neg</sup> cells proliferate slowly and form smaller tumors with poor vascularization. Under hypoxic conditions, the Aldefluor<sup>pos</sup> BCSCs proliferate with high vascularization whereas induced HIF-1 $\alpha$  promotes Aldefluor<sup>neg</sup> cells to become Aldefluor<sup>pos</sup> cells. The data are presented as the means  $\pm$  SD from three independent experiments. \* $P$  < 0.05; \*\* $P$  < 0.01 by Student's *t*-test and by ANOVA with Tukey's multiple comparison test.

Interestingly, Gupta and colleagues showed BCSC-like cells arise *de novo* from non-stem-like cells and explained the cell transition state by a Markov model.<sup>(6)</sup> According to this model, they revealed that interconversion between stem-like fractions and non-stem like fractions (luminal and basal cells) occurs after transplantation *in vivo*.<sup>(7)</sup> In the present study, because Aldefluor<sup>neg</sup> cells partially possess characteristics of BCSCs, it is likely that the magnitude of phenotypic change in CSCs, such as ALDH activity, would be controlled by microenvironmental factors (e.g., hypoxia) and subsequent effects on the epigenetic state of the Aldefluor<sup>neg</sup> population.

In conclusion, hypoxia found in breast cancer tumors is one the most important processes responsible for the induction of HIF-1 $\alpha$  in BCSCs. Consistent with previous reports, it is

suggested that a combination of chemotherapy and HIF-1 $\alpha$  inhibitor would be more effective compared with the current therapy.<sup>(41)</sup> We also predict that inhibition of HIF-1 $\alpha$  that can inhibit ALDH activity in highly hypoxic breast cancer tumor microenvironments will reduce the chances to generate deleterious Aldefluor<sup>pos</sup> BCSCs.

### Acknowledgments

This work was supported by a Grant-in Aid from MEXT, Japan.

### Disclosure Statement

The authors declare no conflict of interest.

### References

- Al-Hajj M, Wicha MS, Benito-Hernandez A *et al.* Prospective identification of tumorigenic breast cancer cells. *Proc Natl Acad Sci USA* 2003; **100**: 3983–8.
- Sheridan C, Kishimoto H, Fuchs RK *et al.* CD44+/CD24– breast cancer cells exhibit enhanced invasive properties: an early step necessary for metastasis. *Breast Cancer Res* 2006; **8**: R59.
- Shipitsin M, Campbell LL, Argani P *et al.* Molecular definition of breast tumor heterogeneity. *Cancer Cell* 2007; **11**: 259–73.
- Ginestier C, Hur MH, Charafe-Jauffret E *et al.* ALDH1 is a marker of normal and malignant human mammary stem cells and a predictor of poor clinical outcome. *Cell Stem Cell* 2007; **1**: 555–67.
- Charafe-Jauffret E, Ginestier C, Iovino F *et al.* Breast cancer cell lines contain functional cancer stem cells with metastatic capacity and a distinct molecular signature. *Cancer Res* 2009; **69**: 1302–13.
- Gupta PB, Fillmore CM, Jiang G *et al.* Stochastic state transition give rise to phenotypic equilibrium in populations of cancer cells. *Cell* 2011; **146**: 633–44.
- Chaffer CL, Brueckmann I, Scheel C *et al.* Normal and neoplastic nonstem cells can spontaneously convert to a stem-like state. *Proc Natl Acad Sci USA* 2011; **108**: 7950–5.
- Zhong H, De Marzo AM, Laughner E *et al.* Overexpression of hypoxia-inducible factor 1 $\alpha$  in common human cancers and their metastases. *Cancer Res* 1999; **59**: 5830–5.
- Xiang L, Gilkes DM, Chaturvedi P *et al.* Ganetespib blocks HIF-1 activity and inhibits tumor growth, vascularization, stem cell maintenance, invasion, and metastasis in orthotopic mouse models of triple-negative breast cancer. *J Mol Med* 2014; **92**: 151–64.
- Sullivan R, Paré GC, Frederiksen LJ *et al.* Hypoxia-induced resistance to anticancer drugs is associated with decreased senescence and requires hypoxia-inducible factor-1 activity. *Mol Cancer Ther* 2008; **7**: 1961–73.
- Chen J, Imanaka N, Griffin JD. Hypoxia potentiates Notch signaling in breast cancer leading to decreased E-cadherin expression and increased cell migration and invasion. *Br J Cancer* 2010; **102**: 351–60.
- Zhu GH, Huang C, Feng ZZ *et al.* Hypoxia-induced snail expression through transcriptional regulation by HIF-1 $\alpha$  in pancreatic cancer cells. *Dig Dis Sci* 2013; **58**: 3503–15.
- Zhang J, Cheng Q, Zhou Y *et al.* Slug is a key mediator of hypoxia induced cadherin switch in HNSCC: correlations with poor prognosis. *Oral Oncol* 2013; **49**: 1043–50.
- Tachi K, Shiraishi A, Bando H *et al.* FOXA1 expression affects to the proliferation activity of luminal breast cancer stem cell populations. *Cancer Sci* 2016; **107**: 281–9.
- Nagano M, Yamashita T, Hamada H *et al.* Identification of functional endothelial progenitor cells suitable for the treatment of ischemic tissue using human umbilical cord blood. *Blood* 2007; **110**: 151–60.
- Nagano M, Kimura K, Yamashita T *et al.* Hypoxia responsive mesenchymal stem cells derived from human umbilical cord blood are effective for bone repair. *Stem Cells Dev* 2010; **19**: 1195–210.
- Morita M, Ohneda O, Yamashita T *et al.* HLF/HIF-2 $\alpha$  is a key factor in retinopathy of prematurity in association with erythropoietin. *EMBO J* 2003; **22**: 1134–46.
- Yang DC, Yang MH, Tsai CC *et al.* Hypoxia inhibits osteogenesis in human mesenchymal stem cells through direct regulation of RUNX2 by TWIST. *PLoS ONE* 2011; **6**: e23965.
- Kobayashi S, Yamashita T, Ohneda K *et al.* Hypoxia-inducible factor-3 $\alpha$  promotes angiogenic activity of pulmonary endothelial cells by repressing the expression of the VE-cadherin gene. *Genes Cells* 2015; **20**: 224–41.
- Emerling BM, Benes CH, Poulogiannis G *et al.* Identification of CDCP1 as a hypoxia-inducible factor 2 $\alpha$  (HIF-2 $\alpha$ ) target gene that is associated with survival in clear cell renal cell carcinoma patients. *Proc Natl Acad Sci USA* 2013; **110**: 3483–8.
- Tomaskova J, Oveckova I, Labudova M *et al.* Hypoxia induces the gene expression and extracellular transmission of persistent lymphocytic choriomeningitis virus. *J Virol* 2011; **85**: 13069–76.
- Yamashita T, Ohneda K, Nagano M *et al.* Hypoxia-inducible transcription factor-2 $\alpha$  in endothelial cells regulates tumor neovascularization through activation of ephrin A1. *J Biol Chem* 2008; **283**: 18926–36.
- Croker AK, Goodale D, Chu J *et al.* High aldehyde dehydrogenase and expression of cancer stem cell markers selects for breast cancer cells with enhanced malignant and metastatic ability. *J Cell Mol Med* 2009; **13**: 2236–52.
- Ponti D, Costa A, Zaffaroni N *et al.* Isolation and in vitro propagation of tumorigenic breast cancer cells with stem/progenitor cell properties. *Cancer Res* 2005; **65**: 5506–11.

- 25 Charafe-Jauffret E, Ginestier C, Iovino F *et al.* Aldehyde dehydrogenase 1-positive cancer stem cells mediate metastasis and poor clinical outcome in inflammatory breast cancer. *Clin Cancer Res* 2010; **16**: 45–55.
- 26 Han M, Wang Y, Liu M *et al.* MiR-21 regulates epithelial-mesenchymal transition phenotype and hypoxia-inducible factor-1 $\alpha$  expression in third-sphere forming breast cancer stem cell-like cells. *Cancer Sci* 2012; **103**: 1058–64.
- 27 Bos R, Zhong H, Hanrahan CF *et al.* Levels of hypoxia-inducible factor-1 alpha during breast carcinogenesis. *J Natl Cancer Inst* 2001; **93**: 309–14.
- 28 Erler JT, Bennewith KL, Nicolau M *et al.* Lysyl oxidase is essential for hypoxia-induced metastasis. *Nature* 2006; **440**: 1222–6.
- 29 Bertout JA, Majnundar AJ, Gordan JD *et al.* HIF2alpha inhibition promotes p53 pathway activity, tumor cell death, and radiation responses. *Proc Natl Acad Sci USA* 2009; **106**: 14391–6.
- 30 Jiang J, Tang YL, Liang XH. EMT: a new vision of hypoxia promoting cancer progression. *Cancer Biol Ther* 2011; **11**: 714–23.
- 31 Jing Y, Han Z, Zhang S *et al.* Epithelial-mesenchymal transition in tumor microenvironment. *Cell Biosci* 2011; **1**: 29.
- 32 Hung SP, Yang MH, Tseng KF *et al.* Hypoxia-induced secretion of TGF- $\beta$ 1 in mesenchymal stem cell promotes breast cancer cell progression. *Cell Transplant* 2013; **22**: 1869–82.
- 33 Sahlgren C, Gustafsson MV, Jin S *et al.* Notch signaling mediates hypoxia-induced tumor cell migration and invasion. *Proc Natl Acad Sci USA* 2008; **105**: 6392–7.
- 34 Leong KG, Niessen K, Kulic I *et al.* Jagged1-mediated Notch activation induces epithelial-to-mesenchymal transition through Slug-induced repression of E-cadherin. *J Exp Med* 2007; **204**: 2935–48.
- 35 Niessen K, Fu Y, Chang L *et al.* Slug is a direct Notch target required for initiation of cardiac cushion cellularization. *J Cell Biol* 2008; **182**: 315–25.
- 36 Conley SJ, Gheordunescu E, Kakarala P *et al.* Antiangiogenic agents increase breast cancer stem cells via the generation of tumor hypoxia. *Proc Natl Acad Sci USA* 2012; **109**: 2784–9.
- 37 Kim RJ, Park JR, Roh KJ *et al.* High aldehyde dehydrogenase activity enhances stem cell features in breast cancer cells by activating hypoxia-inducible factor-2 $\alpha$ . *Cancer Lett* 2013; **333**: 18–31.
- 38 Lu X, Kang Y. Hypoxia and hypoxia-inducible factors: master regulators of metastasis. *Clin Cancer Res* 2010; **16**: 5928–35.
- 39 Gort EH, Groot AJ, van der Wall E *et al.* Hypoxic regulation of metastasis via hypoxia-inducible factors. *Curr Mol Med* 2008; **8**: 60–7.
- 40 Inukai M, Hara A, Yasui Y *et al.* Hypoxia-mediated cancer stem cells in pseudopalisades with activation of hypoxia-inducible factor-1 $\alpha$ /Akt axis in glioblastoma. *Hum Pathol* 2015; **46**: 1496–505.
- 41 Semenza GL. Regulation of the breast cancer stem cell phenotype by hypoxia-inducible factors. *Clin Sci* 2015; **129**: 1037–45.

## Supporting Information

Additional Supporting Information may be found online in the supporting information tab for this article:

**Fig. S1.** Analysis of HIF-2 $\alpha$  protein expression in Aldefluor<sup>neg</sup> BC#1, Aldefluor<sup>pos</sup> BC#1, and Aldefluor<sup>pos</sup>-shHIF-1 $\alpha$  BC#1.

**Fig. S2.** Notch-1 inhibition partially affects EMT in Aldefluor<sup>pos</sup> BC#1 under hypoxic conditions.

**Fig. S3.** The alternation of ALDH activity of Aldefluor<sup>neg</sup> cells under hypoxic conditions.